



ELSEVIER

Surface Science 478 (2001) 1–8



www.elsevier.nl/locate/susc

Initial stages of Sb_2 deposition on $\text{InAs}(001)$

B.Z. Noshov^{a,*}, B.V. Shanabrook^b, B.R. Bennett^b, W. Barvosa-Carter^{b,1},
W.H. Weinberg^a, L.J. Whitman^b

^a Department of Chemical Engineering, University of California, Santa Barbara, CA 93106, USA

^b Naval Research Laboratory, 4555 Overlook Ave. SW, Washington, DC 20375, USA

Received 30 November 2000; accepted for publication 13 February 2001

Abstract

We have used in situ scanning tunneling microscopy to study various preparation techniques for creating InSb bonds on InAs surfaces by molecular beam epitaxy. When an $\text{InAs}(001)-(2 \times 4)$ surface is exposed to an Sb_2 flux, the surface changes to an $\text{InSb}-(1 \times 3)$ -like reconstruction, where one monolayer-deep vacancy islands emerge on the surface due to the change in the composition of the reconstruction. The vacancy islands cannot be annealed out using growth interrupts under Sb_2 . Extended annealing eventually leads to further surface roughening and a change into a reconstruction that may be even more Sb -rich. As the reconstruction changes from the original (2×4) to (1×3) -like, we do not observe any evidence that the vacancy islands form due to material detachment and mass transport from steps. Instead, we find that the vacancy islands develop uniformly across the surface as Sb becomes incorporated into the reconstruction. © 2001 Elsevier Science B.V. All rights reserved.

Keywords: Molecular beam epitaxy; Scanning tunneling microscopy; Surface structure, morphology, roughness, and topography; Antimony; Indium antimonide; Indium arsenide

1. Introduction

Semiconductor heterostructures that contain both arsenides and antimonides have become a subject of much interest. The wide range of band alignments possible with mixed anion heterostructures allows for the fabrication of a variety of applications, including field effect transistors [1], infrared lasers [2], infrared detectors [3], and high-speed oscillators such as resonant tunneling (or

interband tunneling) devices [4–6]. Because the composition and abruptness of the interfaces can affect the performance of some devices [6,7], a critical issue when growing mixed antimonide/arsenide heterostructures by molecular beam epitaxy (MBE) is the formation of high-quality interfaces between the arsenide and antimonide layers. Accordingly, in order to fabricate structures reproducibly, it is important to characterize and understand the evolving surface morphology that arises during the formation of the interfaces.

Three important issues determine the nature of the interfaces in antimonide/arsenide heterostructures. The first issue is the nature of the surface topography present during growth, which may

* Corresponding author.

E-mail address: brett@stm2.nrl.navy.mil (B.Z. Noshov).

¹ Present address: HRL Laboratories, Malibu, CA 90265, USA.

translate into interfacial roughness. For example, islands that evolve on the growth surface might eventually be trapped, causing nanoscale variations in the interfacial structure. The second issue is intermixing among the group V species, which appears as a fluctuation in composition along an interface. Such cross incorporation of atoms at a heterojunction can lead to extended interfaces that may affect the device characteristics (e.g., increased scattering). The third issue is the composition of the interfacial bonds. When III–V heterostructures contain both different cations and anions in adjacent materials, two different types of interfacial bonds can be created to join the layers. For example, in the AlSb/InAs system, either InSb-like or AlAs-like interfacial bonds (or some combination) can be formed depending on the MBE shutter sequence. It has been found generally that InSb-like interfaces are more abrupt and result in better electronic properties than AlAs-like interfaces [8–10]. Some of these effects may be related to the strain associated with the mismatch of the interfacial bonds with the surrounding layers. For example, it has been established previously that the strain from the interfacial bond types in an InAs/GaSb superlattice can change the average lattice constant [11,12]. Because the lattice constants of InSb and AlAs are $\sim 7\%$ larger and smaller, respectively, than that of InAs, the mismatch strain from the interfacial bond types may also influence electronic properties.

Because of the high reactivity of arsenic with antimonide surfaces and the interesting subsequent surface chemistry, there have been a variety of studies of the As-for-Sb exchange reaction associated with arsenic exposures (and InAs growth) on GaSb surfaces, and the compositional abruptness of the resulting interface [13–16]. While similar studies of Sb exposures to InAs surfaces have focused on characterizing any Sb-for-As exchange reaction [15,17], the potential impact of these compositional changes on evolving surface roughness and structure has not been addressed in detail for the Sb-on-InAs case [18]. In this article, we investigate in greater depth the initial stages of Sb₂ exposure and the formation of vacancy islands on the InAs(001) surface using in situ scanning tunneling microscopy (STM).

2. Experimental details

The experiments were performed in an interconnected, multichamber ultrahigh vacuum facility that includes a III–V MBE chamber equipped with a 10 keV electron gun for reflection high-energy electron diffraction (RHEED) and a surface analysis chamber with an STM. The details of the sample mounting and transfers have been described previously [19]. All samples were grown with no intentional doping using “cracked” As₂ and Sb₂ sources on InAs(001) “epi-ready” wafers. Following oxide removal, a ~ 0.5 μm -thick film of InAs was grown at 1 ML/s, with an As-to-In true flux ratio of 2:1, and 30 s interrupts under As₂ every 90 s. The growth temperature was estimated to be $\sim 470^\circ\text{C}$. In order to produce atomically flat and well-ordered InAs surfaces, a 10 min growth interrupt was performed at the conclusion of the growth. The As₂ flux was periodically reduced throughout this interrupt, during which time the RHEED pattern progressed from a streaky (2×4) to sharp diffraction spots along each streak. The samples were cooled to various temperatures below the InAs growth temperature prior to Sb₂ exposure. The beam equivalent pressure of Sb₂ was kept constant at $\sim 2.5 \times 10^{-6}$ Torr for all exposures. As the sample temperature was being lowered, the samples were rotated away from the sources to minimize any exposure to unintentional leakage from the shuttered sources. Once the temperature stabilized, the samples were rotated back to face the sources and resume deposition.

After each growth was completed, the sample was immediately removed from the MBE chamber and transferred in vacuo to the analysis chamber. The base pressure in the transfer section was $< 5 \times 10^{-10}$ Torr, and the entire transfer process typically took about 5 min to complete. The samples were then allowed to cool to room temperature (about 1 h in a background pressure $< 1 \times 10^{-10}$ Torr) before imaging with the STM. All STM images shown here were acquired in constant-current mode with sample biases ranging from -2 to -3 V and tunneling currents between 30 pA and 1 nA. Note that the images have not been corrected for thermal drift.

3. Results and discussion

The InAs(001) buffer layer is nearly ideal, composed of large (2×4)-reconstructed terraces that are atomically smooth and separated by monolayer height (0.3 nm) steps, as shown in Fig. 1(a). Larger scale images presented elsewhere [18] show that the terraces are typically ~ 0.1 – $0.5 \mu\text{m}$ wide with essentially no islands, with the step density determined by the local surface misorientation from (001). At higher magnification (inset), the atomic scale structure characteristic of the established $\beta 2(2 \times 4)$ reconstruction is observed [20–22]. The (2×4) reconstruction is highly ordered with relatively few defects, in agreement with the sharp diffraction spots observed in RHEED at the end of the InAs growth.

When an InAs(001)-(2×4) surface is exposed to an Sb_2 flux, the surface bifurcates such that vacancy islands cover $\sim 25\%$ of the surface [18]. A large-scale image of an InAs surface exposed to an Sb_2 flux for 2 s (~ 5 Langmuirs (L)) at a substrate

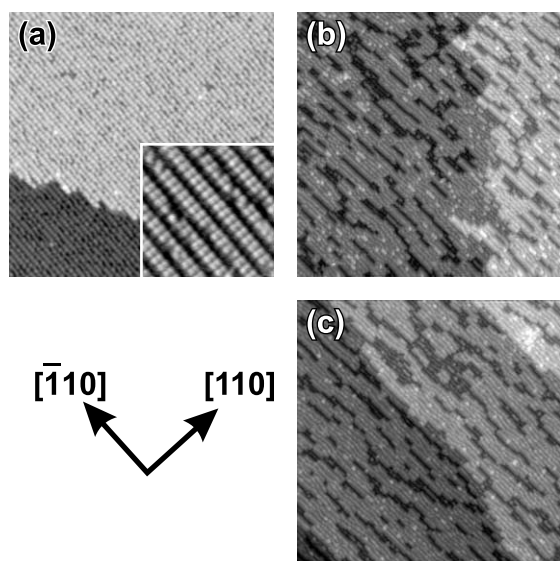


Fig. 1. Filled-state STM images ($85 \times 85 \text{ nm}^2$) of (a) a clean InAs(001)- $\beta 2(2 \times 4)$ surface; (b) a surface exposed to Sb_2 for 2 s at $\sim 2.5 \times 10^{-6}$ Torr with a substrate temperature $\sim 400^\circ\text{C}$; and (c) a similar surface after depositing 1 ML of In followed by 2 s of Sb_2 . The inset in (a) shows a higher magnification view of the (2×4) reconstruction. The vacancy islands in (b) and (c) both cover $\sim 25\%$ of the surface.

temperature of $\sim 400^\circ\text{C}$ is shown in Fig. 1(b). For comparison, an image of the surface prepared by migration-enhanced epitaxy (MEE) is shown in Fig. 1(c). For the MEE-prepared sample, the InAs(001)-(2×4) surface was first exposed to 1 ML of In followed by 2 s of Sb_2 ; again, vacancy islands cover $\sim 25\%$ of the surface. Both surfaces exhibit a disordered (1×3)-like reconstruction on the terraces and in the vacancy islands, consistent with the streaky RHEED patterns observed immediately after the Sb_2 exposure. We have shown previously that the vacancy islands form because of the different compositions of the As-terminated $\beta 2(2 \times 4)$ and the Sb-terminated (1×3)-like reconstructions [23,24].

There are no apparent differences in the (1×3)-like reconstructions formed using Sb_2 exposures versus MEE, and the STM images are similar in appearance to those previously observed for similar Sb-rich reconstructions on other III–Sb(001) surfaces (including InSb) [25–29]. However, it is important to note that the atomic-scale composition of the reconstructions may not be precisely the same; for example, subtle variations in the amount of Sb vs. As in the surface structure can be difficult to distinguish in plan-view STM images. A higher magnification image of the reconstruction on an MEE-prepared surface is shown in Fig. 2. The reconstruction appears as rows of dimer-like structures (illustrated in black), sometimes separated by rotated dimer-like features at a lower height (in white). Note that along the top-layer dimer rows there are occasional “notches”, where it appears that one-half a dimer is missing (a few are circled). These structures are periodic on homoepitaxial AlSb and GaSb(001)- $\beta(4 \times 3)$ surfaces [28], where they have been shown to be mixed III–Sb “heterodimers”. The InSb-(1×3)-like reconstruction observed here generally resembles the $\beta(4 \times 3)$ reconstruction, which is terminated by $1\frac{7}{12}$ ML of Sb plus $1/12$ ML of surface group III atoms [28]. In this case, however, the heterodimers are not well ordered, and occur at a much lower density, suggesting the reconstruction is similar but may not have a full $1/12$ ML of In in the top layer. In the absence of periodic heterodimers, the InSb-like MEE surface reconstruction is actually more of a (2×3)-like or $c(2 \times 6)$ reconstruction

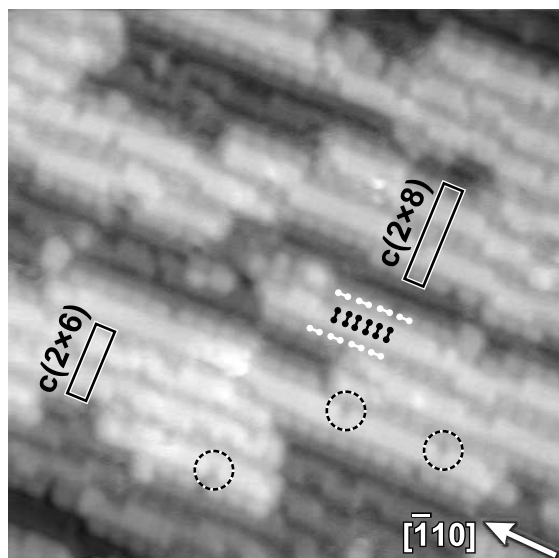


Fig. 2. Filled-state STM image ($18 \times 18 \text{ nm}^2$) showing a higher magnification view of the InAs surface exposed to 1 ML of In and 2 s of Sb_2 (cf. Fig. 1(c)). A $c(2 \times 6)$ unit cell has been outlined and a ball-and-stick model shown over a $c(2 \times 6)$ area illustrates the locations and orientations of dimers on the reconstructed surface. The top-layer Sb dimers are shown in black and the second-layer dimers in white. A $c(2 \times 8)$ unit cell has also been outlined illustrating the slightly different reconstruction when an extra row of second-layer Sb dimers is present.

because of the alignment of the rotated dimers in the second layer [18,25]. A simple model showing the location of the top-(black) and second-layer (white) Sb dimers in Fig. 2 illustrates how the ordering of these dimers can make a local $c(2 \times 6)$ structure. In this particular image, we also observe some areas where there is an extra row of second-layer Sb dimers between the top-layer dimer rows, creating regions with a (2×4) -like or $c(2 \times 8)$ -like reconstruction (depending again on the alignment of the second-layer dimers). This arrangement occurs naturally within a disordered (1×3) -like structure when a kink occurs in a top dimer row, shifting it by a lattice constant in the $[110]$ direction.

We have shown previously that when using MEE to form the interfacial bonds, the initial 1 ML of In traps the surface As and inhibits possible displacement by Sb [30]. After the In deposition, exposure to Sb_2 forms the InSb-like (1×3)

structure with presumably $\sim 1\frac{7}{12}$ ML of Sb. However, when an InAs(001)- $\beta 2(2 \times 4)$ surface is exposed directly to Sb_2 , the Sb could incorporate into the surface reconstruction via various pathways. Although our STM results do not offer any direct insight into the chemical composition within the InSb-like reconstruction, we note that in related work Wang et al. have observed that the As-to-In peak intensity ratio in X-ray photoelectron spectroscopy decreases when InAs surfaces are exposed to Sb_2 . The authors concluded that an exchange reaction does indeed occur, and that the majority of the surface As is displaced during a 5 s Sb_2 exposure [15]. One mechanism for such displacement involves the Sb-induced breaking of InAs bonds to form InSb bonds; although, from an energetics perspective, the formation of InSb bonds via anion exchange of Sb-for-As is not favorable based on the relative free energies of formation and the bond strengths [9]. An alternative mechanism involves As desorbing from the surface to momentarily form a group III-rich reconstruction, such that Sb can replace the desorbed As and incorporate into the reconstruction. We might expect that given enough time under exposure to an Sb_2 flux, the original surface As could eventually be displaced by Sb via this mechanism given the constant desorption and adsorption of group V species. Note, however, that at 400°C the InAs(001)- (2×4) reconstruction is relatively stable in vacuum, and does not lose surface As via desorption over the time scales of these Sb_2 exposures. A third and perhaps more likely mechanism is that Sb could attach directly to the In atoms beneath the As dimers on the (2×4) reconstruction. In this scenario, the preferential adsorption sites would be between the dimer rows – i.e., along the “missing row” of group III atoms within the $\beta 2(2 \times 4)$ structure – where the Sb could react with the exposed In dangling bonds. Because the (1×3) structure is similar to the $\beta(4 \times 3)$ models, we suspect that the surface would be terminated with $\sim 1\frac{7}{12}$ ML of group V. However, it is not clear if the original As has been displaced from the surface, or rather has been incorporated into the (1×3) reconstruction. Indeed, well-ordered reconstructions containing both As and Sb surface dimers have been observed previously with only

subtle features that might indicate the dimer composition [31].

A common technique employed to produce smooth, island-free surfaces during MBE is to use growth interrupts, i.e., annealing in the presence of a group V flux. After exposing an InAs(001)-(2 × 4) surface to an Sb₂ flux, a growth interrupt under Sb₂ was performed to try to “anneal out” the islands (presumably via coalescence into the step edges). For interrupt times up to 5 min at ~400°C, we found that an interrupt does not significantly change the surface roughness: a two-level surface remains with vacancy islands still covering ~25% of the surface. There is a slight change in the vacancy island shape and density, indicating that some degree of diffusion and coalescence has occurred, but there is no evidence of a net incorporation of the vacancy islands into the steps. They still appear uniformly distributed across the surface.

Annealing at a higher temperature (~480°C) under Sb₂ for 10 min, however, dramatically changes the surface, as shown in Fig. 3(a). (Note that a substrate step edge runs vertically up the center of this image.) The most notable change in the surface is the emergence of highly anisotropic islands elongated in the $[\bar{1}10]$ direction. On each substrate terrace, there are now three different levels separated by monolayer-height steps. The vacancy islands have become highly elongated, appearing as dark streaks between new, monolayer-height islands that are uniformly three to four (1 × 3)-unit cells wide (4–5 nm). It is interesting that instead of causing the vacancy islands to coalesce into the steps, annealing under Sb₂ has caused the surface to roughen further: *the vacancy islands cannot simply be annealed out.* (Note that some Sb₂ flux is required at this temperature to prevent the surface from going group III rich.) The additional roughness may be a consequence of strain from the ~7% larger lattice of the InSb-like interfacial bonds. As observed in other III–V heteroepitaxial systems, including (In,Ga,Al)Sb/GaAs [32,33] and In(Ga)As/GaAs [34,35], island formation (i.e., surface roughening) can serve as a strain-relief mechanism that lowers the surface free energy. A higher temperature and longer annealing time may enable the Sb/InAs surface to

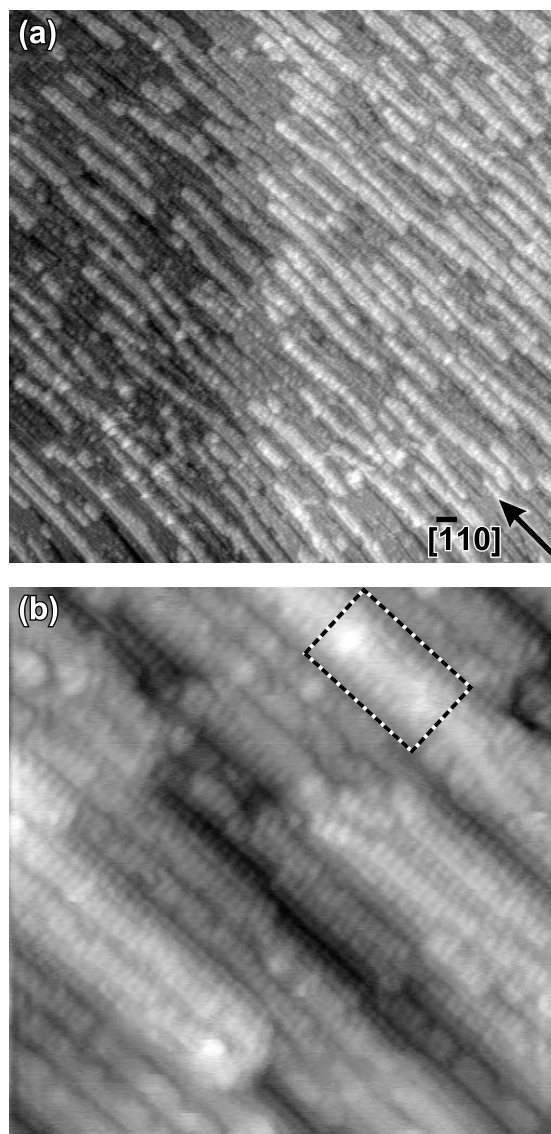


Fig. 3. Filled-state STM images of an InAs surface after exposure to Sb₂ for 10 min at 480°C. The image sizes are (a) 250 × 250 nm² and (b) 18 × 18 nm². The long interrupt under Sb₂ has caused the surface to roughen and form monolayer-height islands in addition to the vacancy islands. The outlined area in (b) highlights a structure similar to a (2 × 8) reconstruction observed when GaAs(001) is annealed in Sb.

overcome kinetic barriers and form this possibly lower energy morphology. The ribbon-like “islands” in Fig. 3 are also very similar to those observed following sub-monolayer InAs growth on

GaAs(001)-(2 × 4) [35,36]. Given that the nominal lattice mismatch of InSb/InAs is nearly the same as InAs/GaAs, this similarity further supports our belief that the terminal layer is InSb-like.

A higher magnification image of the surface formed by the long, high-temperature interrupt is shown in Fig. 3(b). Although much of the surface exhibits a disordered (1 × 3)-like reconstruction, we again observe some areas that give a (2 × 4)-like structure. The outlined area in Fig. 3(b) highlights yet another structure sometimes seen. This structure has a multilevel appearance that strongly resembles an Sb-rich (2 × 8) reconstruction formed when GaAs(001)-β2(2 × 4) experiences a prolonged exposure to Sb, a structure that includes ~1 ML of Sb [31].

We have tried to determine the mechanisms underlying vacancy island formation by exposing a well-ordered InAs(001)-β2(2 × 4) surface to a relatively small amount of Sb₂, a ~0.5 s exposure (~1.25 L), at a substrate temperature of ~400°C. Images of the resulting surface are displayed in Fig. 4. The Sb appears to adsorb uniformly across the surface as patches or clusters on top of the (2 × 4) reconstruction. There does seem to be a slightly higher density of clusters at the step edge [cf. Fig. 4(a)], possibly indicating a faster reaction rate at step edges. Note that one way a bilvel surface might be expected to form is for material to detach from steps and create islands nearby on the adjacent terrace. If this were the case, however, one would expect to see a concentration of small islands on the *lower side* of the step edges, which appears to rule out such a mechanism.

Higher magnification images of the briefly exposed surface are shown in Fig. 4(b) and (c). At this low an exposure, we can begin to see how the (2 × 4) reconstruction becomes disordered via defect accumulation. In addition to causing As vacancy-like structures, the Sb adsorption also generates many small protrusions that are presumably Sb clusters. As highlighted in Fig. 4(c), it appears that the Sb initially adsorbs in the trench between the rows of the β2(2 × 4) reconstruction. This observation is consistent with our earlier conjecture that Sb might initially bond directly to the In on the surface, as opposed to first displacing As. A similar example of preferential adsorption

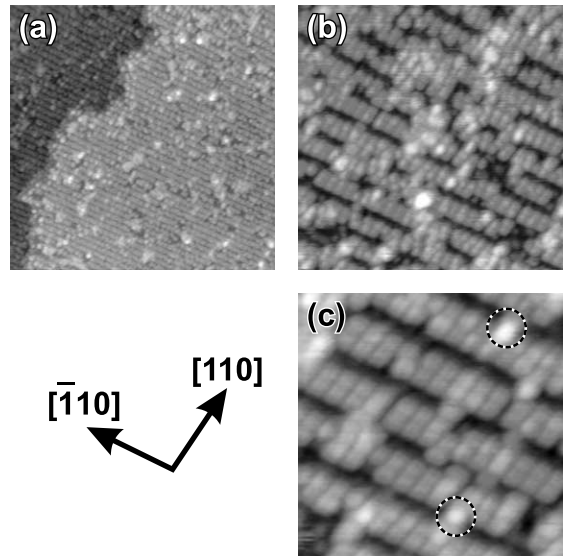


Fig. 4. Filled-state STM images of InAs surfaces exposed to 0.5 s of Sb₂ at 400°C. The image sizes are (a) 75 × 75 nm², (b) 18 × 18 nm², and (c) 9 × 9 nm².

in the trench sites has been reported for Br/GaAs(001)-β2(2 × 4) [37]. It is believed that the impinging group V species are nominally repelled from the surface As dimers and directed towards the trench where they can interact directly with the In dangling bonds.

We have also tried to capture the initial stages of Sb adsorption by observing the effects of adsorption at lower substrate temperatures where surface reactions will occur more slowly. Fig. 5 displays an image of an InAs surface exposed to Sb₂ for 2 s at the same flux as above, but with a substrate temperature ~300°C (100°C cooler). These conditions cause a very interesting surface morphology with an extremely disordered, complex, anisotropic structure. Long-range order is no longer observed in the reconstruction, and small vacancy-like patches have appeared that perhaps are the beginnings of vacancy islands. There are many string-like features oriented along the [110] direction that could be remnants of the original (2 × 4) reconstruction, the initial formation of the (1 × 3)-like reconstruction, or some combination of both. Additional Sb₂ exposure at ~300°C leads to a more ordered (1 × 3) structure, and eventually

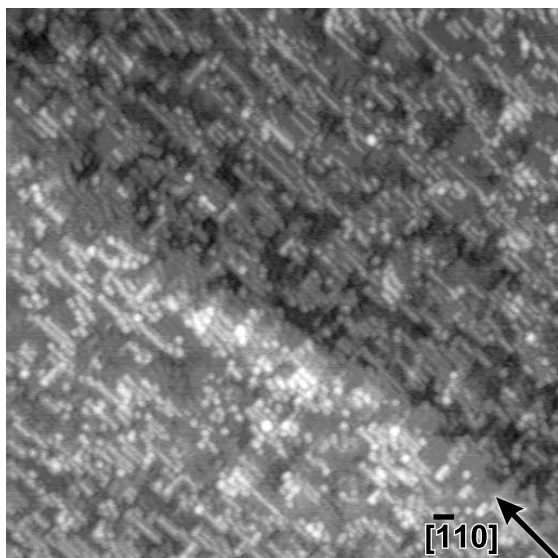


Fig. 5. Filled-state STM image ($75 \times 75 \text{ nm}^2$) of an InAs surface exposed to Sb_2 for 2 s at 300°C . The surface is complex and highly disordered.

a (1×5) structure after ~ 45 s. These results indicate that the reaction of Sb with InAs occurs relatively uniformly across the surface.

The initial disordering of the surface upon Sb_2 exposure is consistent with the sudden decrease in signal intensity observed concomitantly by RHEED [17]. During further exposure, the RHEED specular intensity eventually recovers to a new steady-state value as the (1×3) pattern develops. Collins et al. compared RHEED and X-ray photoelectron spectroscopy data and showed that when the intensity of the specular spot was at a minimum, the Sb coverage was not yet at its saturation value [17]. This is consistent with our results, which indicate that at the point of maximum disorder, the reconstruction transition is still evolving and the surface anion composition is likely a mixture of As and Sb. Presumably, as more Sb is added and the transition continues, the Sb-terminated surface begins to order into the InSb- (1×3) -like structure, at which time the intensity of the RHEED specular spot recovers. Hence, the observed modulation in the RHEED intensity appears to be indicative of the phase transition between the surface reconstructions.

4. Conclusions

We have studied the initial stages of Sb_2 exposure on InAs (001) - $\beta_2(2 \times 4)$ as a means of creating InSb-like bonds on the surface. The exposure to Sb_2 causes the surface reconstruction to change from the original As-terminated (2×4) to a (1×3) reconstruction similar to what is commonly observed on Sb-terminated III–Sb (001) surfaces. Because the reconstructions have different III/V compositions, exposure to Sb_2 causes the formation of vacancy islands that cover $\sim 25\%$ of the surface. The Sb adsorbs on the InAs surface in an anion exchange and/or incorporation reaction to form InSb bonds, with the initial adsorption appearing to occur in the (2×4) trenches. As InSb surface bonds are formed, an InSb- (1×3) -like reconstruction emerges. Because of the significant mass transport required, the surface initially becomes highly disordered. The reaction nucleates uniformly across the surface, with substrate step edges having little effect. The resulting vacancy islands are very stable, and cannot be “annealed out”, possibly because of kinetic or strain limitations. Unexpectedly, we find that prolonged annealing under Sb_2 actually causes further surface roughening accompanied by the formation of a complex, highly anisotropic surface structure.

Acknowledgements

This work was supported by the Office of Naval Research, the Defense Advanced Research Projects Agency, and QUEST (an NSF Science and Technology Center for Quantized Electronic Structures, grant no. DMR 91-20007).

References

- [1] J.B. Boos, B.R. Bennett, W. Kruppa, D. Park, M.J. Yang, B.V. Shanabrook, *Electron. Lett.* 34 (1998) 403.
- [2] M.J. Yang, W.J. Moore, B.R. Bennett, B.V. Shanabrook, *Electron. Lett.* 34 (1998) 270.
- [3] F. Fuchs, U. Weimer, W. Pletschen, J. Schmitz, E. Ahlswede, M. Walther, J. Wagner, *Appl. Phys. Lett.* 71 (1997) 3251.

- [4] J.S. Scott, J.P. Kaminski, S.J. Allen, D.H. Chow, M. Lui, T.Y. Liu, *Surf. Sci.* 305 (1994) 389.
- [5] E.R. Brown, E.R. Söderström, J.R. Parker, L.J. Mahoney, K.M. Molvar, T.C. McGill, *Appl. Phys. Lett.* 58 (1991) 2291.
- [6] J.R. Söderström, E.R. Brown, C.D. Parker, L.J. Mahoney, J.Y. Yao, T.G. Andersson, T.C. McGill, *Appl. Phys. Lett.* 58 (1991) 275.
- [7] P. Roblin, R.C. Potter, A. Fathimulla, *J. Appl. Phys.* 79 (1996) 2502.
- [8] B.R. Bennett, B.V. Shanabrook, E.R. Glaser, *Appl. Phys. Lett.* 65 (1994) 598.
- [9] J. Schmitz, J. Wagner, F. Fuchs, N. Herres, P. Koidl, J.D. Ralston, *J. Cryst. Growth* 150 (1994) 858.
- [10] B. Brar, J. Ibbetson, H. Kroemer, J.H. English, *Appl. Phys. Lett.* 64 (1994) 3392.
- [11] B.R. Bennett, B.V. Shanabrook, R.J. Wagner, J.L. Davis, J.R. Waterman, *Appl. Phys. Lett.* 63 (1993) 949.
- [12] J. Wagner, J. Schmitz, N. Herres, F. Fuchs, D. Serries, B. Grietens, S. Németh, C.V. Hoof, G. Borghs, *Physica E* 2 (1998) 320.
- [13] Q. Xie, J.E.V. Nostrand, J.L. Brown, C.E. Stutz, *J. Appl. Phys.* 86 (1999) 329.
- [14] R. Kaspi, *J. Cryst. Growth* 201/202 (1999) 864.
- [15] M.W. Wang, D.A. Collins, T.C. McGill, R.W. Grant, *J. Vac. Sci. Technol. B* 11 (1993) 1418.
- [16] M.W. Wang, D.A. Collins, T.C. McGill, R.W. Grant, R.M. Feenstra, *J. Vac. Sci. Technol. B* 13 (1995) 1689.
- [17] D.A. Collins, M.W. Wang, R.W. Grant, T.C. McGill, *J. Vac. Sci. Technol. B* 12 (1994) 1125.
- [18] B.Z. Noshu, W.H. Weinberg, J.J. Zinck, B.V. Shanabrook, B.R. Bennett, L.J. Whitman, *J. Vac. Sci. Technol. B* 16 (1998) 2381.
- [19] L.J. Whitman, P.M. Thibado, F. Linker, J. Patrin, *J. Vac. Sci. Technol. B* 14 (1996) 1870.
- [20] C. Ratsch, W. Barvosa-Carter, F. Grosse, J.H.G. Owen, J.J. Zinck, *Phys. Rev. B* 62 (2000) R7719.
- [21] Q. Xue, T. Hashizume, T. Sakurai, *Prog. Surf. Sci.* 56 (1998) 1.
- [22] V.P. LaBella, H. Yang, D.W. Bullock, P.M. Thibado, *Phys. Rev. Lett.* 83 (1999) 2989.
- [23] B.Z. Noshu, W.H. Weinberg, W. Barvosa-Carter, B.R. Bennett, B.V. Shanabrook, L.J. Whitman, *Appl. Phys. Lett.* 74 (1999) 1704.
- [24] B.Z. Noshu, W.H. Weinberg, W. Barvosa-Carter, A.S. Bracker, R. Magno, B.R. Bennett, J.C. Culbertson, B.V. Shanabrook, L.J. Whitman, *J. Vac. Sci. Technol. B* 17 (1999) 1786.
- [25] M.T. Sieger, T. Miller, T.-C. Chiang, *Phys. Rev. B* 52 (1995) 8256.
- [26] U. Resch-Esser, N. Esser, B. Brar, H. Kroemer, *Phys. Rev. B* 55 (1997) 15401.
- [27] P.M. Thibado, B.R. Bennett, B.V. Shanabrook, L.J. Whitman, *J. Cryst. Growth* 175/176 (1997) 317.
- [28] W. Barvosa-Carter, A.S. Bracker, J.C. Culbertson, B.Z. Noshu, B.V. Shanabrook, L.J. Whitman, H. Kim, N.A. Modine, E. Kaxiras, *Phys. Rev. Lett.* 84 (2000) 4649.
- [29] C.F. McConville, T.S. Jones, F.M. Leibsle, S.M. Driver, T.C.Q. Noakes, M.O. Schweitzer, N.V. Richardson, *Phys. Rev. B* 50 (1994) 14965.
- [30] B.Z. Noshu, W. Barvosa-Carter, M.J. Yang, B.R. Bennett, L.J. Whitman, *Surf. Sci.* 465 (2000) 361.
- [31] L.J. Whitman, B.R. Bennett, E.M. Kneeder, B.T. Jonker, B.V. Shanabrook, *Surf. Sci.* 436 (1998) L707.
- [32] B.R. Bennett, B.V. Shanabrook, P.M. Thibado, L.J. Whitman, R. Magno, *J. Cryst. Growth* 175/176 (1997) 888.
- [33] B.R. Bennett, P.M. Thibado, M.E. Twigg, E.R. Glaser, R. Magno, B.V. Shanabrook, L.J. Whitman, *J. Vac. Sci. Technol. B* 14 (1996) 2195.
- [34] D. Leonard, M. Krishnamurthy, C.M. Reaves, S.P. DenBaars, P.M. Petroff, *Appl. Phys. Lett.* 63 (1993) 3203.
- [35] V. Bressler-Hill, S. Varma, A. Lorke, B.Z. Noshu, P.M. Petroff, W.H. Weinberg, *Phys. Rev. Lett.* 74 (1995) 3209.
- [36] V. Bressler-Hill, A. Lorke, S. Varma, K. Pond, P.M. Petroff, W.H. Weinberg, *Phys. Rev. B* 50 (1994) 8479.
- [37] Y. Liu, A.J. Komrowski, A.C. Kummel, *Phys. Rev. Lett.* 81 (1998) 413.